STRUCTURAL AND OPTICAL INVESTIGATIONS OF LOW TEMPERATURE SOLUTION BASED SYNTHE-SIZED ZnO AND Ag ADMIX ZnO NANOPARTICLES (NPs)

Jai Singh[*], P. Kumar, R.S. Tiwari, O.N. Srivastava

Dept. of Physics, Faculty of Science, Banaras Hindu University, 221005, Varanasi, India

ABSTRACT

Looking at huge range of applications of nanostructures, ZnO is being considered as technological material. Simple and green production techniques for ZnO and other nanostructured material can enhance the detection of its unusual properties. In this context water-based wet chemical synthesis process for nanostructured ZnO and Ag admixed ZnO nanocrystals has explored in present work. A high yield of the ZnO and Ag admixed ZnO nanocrystals with different Ag contents is successfully synthesized through a simple wet chemical method at the low temperatures in the absence of any surfactants/template. The as synthesized products has been characterized by X-ray diffraction (XRD), transmission electron microscopy (TEM), Fourier transform IR (FTIR), UV-VIS spectroscopy, and photoluminescence spectroscopy. The size of the nanoparticles is found to increase with the increase in Ag content. Large blue-shifts relative to the bulk exciton absorption are observed in the absorption and PL spectra in the pure and Ag admixed ZnO. The emission intensity of PL of Ag admixed ZnO has been found to decrease considerably with respect to that of pure ZnO. NaOH plays multiple roles in the formation of pure and Ag admix ZnO NPs.

Key words: ZnO nanoparticles, TEM, PL, Wet chemical.

INTRODUCTION

ZnO as a versatile II–VI semiconductor material has a multiplicity in applications counting field effect transistors, gas sensors, field emitter, piezoelectric devices and solar cells [1-5]. Considering the applications in optics and catalysis, more interests have been aroused for constructing ZnO nanostructures, including noble metal/ZnO hollow nanoparticles [6], Pt/ZnO porous nanocages [7], ZnO-based core/shell (ZnO/ZnS, ZnO/Ag_2S, and ZnO/CuS) microspheres [8], and Co_3O_4/ZnO hetero-structured nano-wires [9]. Especially, ZnO/Ag nanostructures with various morphologies have been obtained with different synthesis strategies, such as dendrite-like Ag/ZnO hetero-structure nano-crystals [10-13] and a unique dimer-type hetero-structure of Ag/ZnO nanofibers [14].

---

[*] e-mail: jai.bhu@gmail.com

In the present work, ZnO and Ag admixed ZnO nanoparticles have been fabricated by simple solution method using zinc and silver precursors. In comparison to the other techniques, solution method offers simplicity in the process of synthesis with good control on size and capable of providing advantages such as convenient replacement of source. The structural and optical properties of these nanoparticles have also been investigated.

All chemicals were of AR grade purchased from Merck, Germany and used as such without further purification. In a representative synthesis of ZnO, (0.005M) zinc nitrate (ZnNO$_3$ 6 H$_2$O) was taken with 100 ml 0.001 M NaOH solution and stirred for ~60 min at 70 °C. Similar process was adopted for the synthesis of Ag (0.5 and 1 at. %) admixed ZnO NPs through introducing silver nitrate (AgNO$_3$) in the above solution. Finally, the precipitates were collected and washed with anhydrous ethanol and hot distilled water for several times, then dried in vacuum at 120 °C for 2 hrs. The obtained products were examined under scanning electron microscopy, transmission electron microscopy and X-ray diffractometer. For TEM observations, the products were ultrasonically dispersed in ethanol and then dropped onto carbon-coated copper grid. TEM observations were carried out on high resolution transmission electron microscope (HRTEM, Tecnai 20 G^2 FEI). The XRD analyses were performed on a Philips X'PERT PRO PAN Analytical X-ray diffractometer with CuKα irradiation (wavelength, $\lambda = 1.5406$ Å) at a scanning speed of 0.02° s^{-1}. The photoluminescence (PL) spectrum at room temperature was measured by a PerkinElmer LS 55 luminescence spectrometer. The optical absorption properties of the as synthesized samples were measured using a PerkinElmer Lambda-750S UV-Vis spectrophotometer.

STRUCTURAL, OPTICAL AND MORPHOLOGICAL CHARACTERIZATIONS

Fig. 1 shows the XRD patterns of the as synthesized ZnO and Ag admixed ZnO samples having characteristic lines corresponding to (10.0), (00.2), (10.1), (11.0) and (11.2) planes of wurtzite hexagonal ZnO structure. As expected, the XRD peaks of ZnO and Ag admixed ZnO samples were considerably broadened compared to bulk material due to small size of the NPs. The size of the crystallites were estimated using Scherrer formula

$$A = 0.94\lambda/\beta\cos\theta, \qquad (1)$$

where A, is the crystallite size, β the full-width-at-half-maximum (FWHM) of the diffraction peak, λ (1.5406 Å) is the wavelength of X-ray radiation and θ is the angle of diffraction. The average crystallite size of ZnO and Ag admixed ZnO samples were found to be in the range of ~ 8 - 12 nm. UV-Visible absorption spectra of as-synthesized ZnO and Ag admixed ZnO samples are illustrated in *Fig. 2a*.
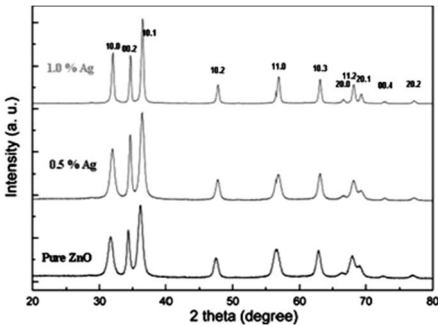
Fig. 1 – X-ray diffraction of as synthesized
ZnO and Ag admixed ZnO

The absorption maximum was found at 300 nm for pure ZnO. On admixing of Ag, the ZnO absorption band has been found red shifted along with the slight decrease in optical density and FWHM that may because of an increase in size of the nano-crystals. The absorption spectrum was studied without taking into account the reflection and trans-mission losses. For pure and admixed ZnO NPs, a sharp ab-sorption edge close to the 350 nm is observed which is believed to arise from the absorption of the near band edge free excitons. Since the average diameter of the particles is in the quantum-confinement regime so it is expected to show a large blue-shift in the absorption bands of ZnO nanoparticles.
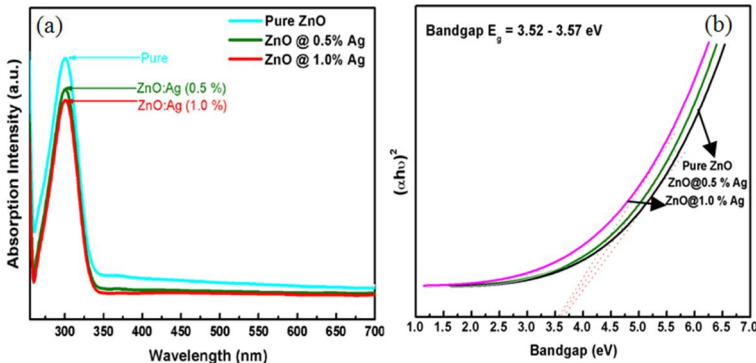

Fig. 2 – a – UV-Visible absorption spectra of as synthesized pure and Ag admixed ZnO at room temperature;. b – Band gap of as synthesized pure and Ag admixed ZnO at room temperature.

The absorption data were analyzed using the classical relation for near the edge optical absorption of semiconductor

$$\alpha = (h\nu - E_g)^{n/2}/h\nu, \tag{1}$$

where h is a constant, E_g is the optical band gap and n is a constant equal to 1 for direct band gap semiconductor and 4 for indirect gap semiconductor materials [39]. The variation of $(\alpha h\nu)^2$ versus hν is linear at the absorption edge which confirms the direct band gap transition in ZnO. Extrapolating the

straight-line portion of the plot to zero absorption coefficient value gives the direct band gap E_g. The band gap energy (E_g) of ZnO and Ag admixed ZnO samples are found to be 3.57 eV (~350 nm) and 3.52 eV (~356 nm), respectively as shown in *Fig 2b*. It means a large shift from 3.57 eV to 3.52 eV that showed the large 'blue shift' of 0.20 - 0.15 eV from standard bulk band gap at room temperature (E_g = 3.37 eV). This blue shift with respect to pure ZnO can be explained on account of quantum size effect (due to the electron hole confinement in a small volume). Admixing of silver in the ZnO sample reduces the optical density and FWHM due to involvement of some ground state week interaction/perturbation of electronic states of ZnO due to the presence of silver particles.
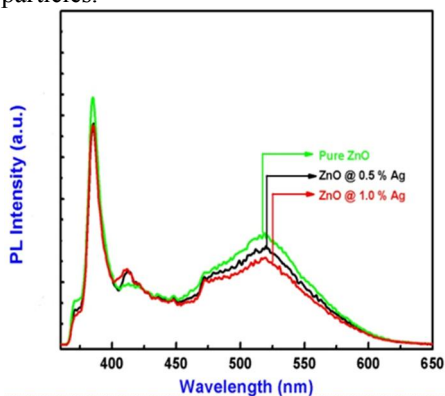

Fig. 3 – PL spectra of as synthesized ZnO and Ag admixed ZnO at room temperature

Emission spectrum of the samples was recorded upon excitation at 325 nm. This excitation wavelength corresponds to the absorption onset detected in the UV-Visible spectra. The room temperature PL spectra of as-synthesized ZnO and Ag admixed ZnO samples are shown in *Fig. 3*. The emission band centered around 385 nm is attributed to the recombination of excitons and the green emission resulting from the recombination of photon-generated holes with charge states of the specific defects. The intensity of the green emission peak at 511 nm which arises due to the defects states in the ZnO, slightly decreases as Ag content increase. This decrease in 511 nm emission band intensity may be attributed to the effect of the Ag that improves the separation between the photo induced electrons and holes [15]. A low intensity blue emission at 415 nm originates from some interface traps of radiative defects at the grain boundaries between silver and ZnO grains. The emission peaks are found red-shifted corresponding to the absorption peak. A similar size dependent red-shift in the PL emission with respect to optical absorption has been observed for ZnSe quantum dots. A recent report on ZnSe/ZnS quantum dots by Nikesh and Mahamuni has also shown a large non resonant PL stokes shift of 220-690 meV for 28-15 nm diameter ZnSe/ZnS quantum dots [16]. *Fig. 4*(a & b) represents TEM micrograph of pure ZnO NPs. It is revealed from TEM micrograph that the size of the NPs is in the range 5-10 nm. HRTEM picture of the crystallites recorded in order to resolve the lattice planes. *Fig. 4c* represents HRTEM micrograph of pure ZnO Nps which shows the highly crystalline nature of the sample. The

interplanner separation (d) obtained from the HRTEM micrograph is $d = 2.60$ Å along (00.2) plane of ZnO. The selected area electron diffraction (SAED) pattern of these nanocrystals is shown in *Fig. 4d*. As expected, in the case of nanocrystals, the electron diffraction patterns show a set of rings instead of spots due to the random orientations of the nanocrystallites, corresponding to the diffraction from different atomic planes of the nanocrystallites and the SADP of ZnO with [10.0], [00.2], [11.0] and [10.1] diffraction planes of ZnO hexagonal structure.
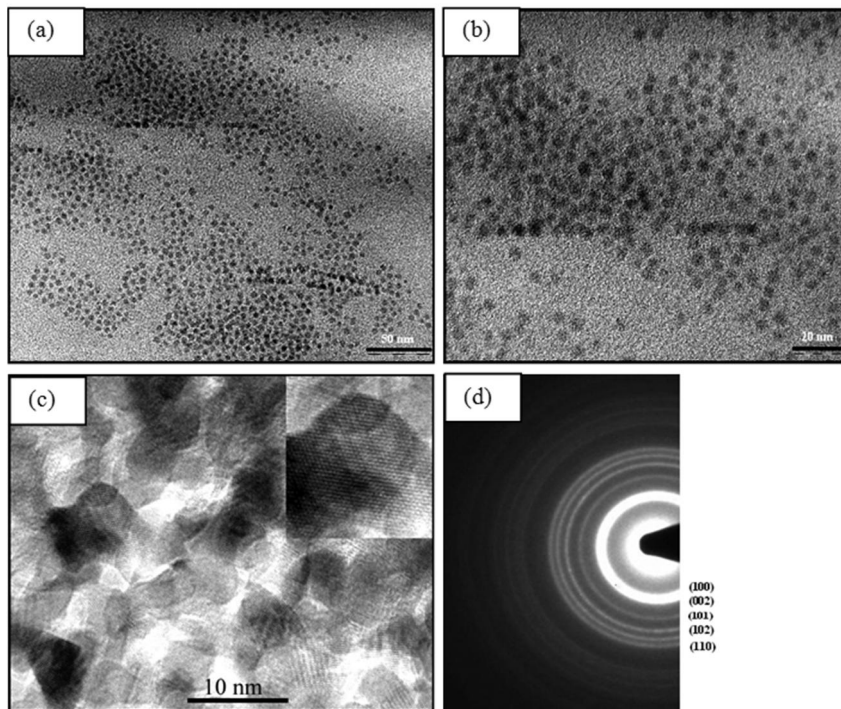

Fig.4 –*a, b* – TEM images of as synthesized ZnO NPs; c – HRTEM image of ZnO Nps; d – selected area diffraction of ZnO NPs

Fig. 5a represents the TEM micrograph of 0.5 % at. Ag admixed ZnO NPs. The average size of the nanoparticles has found to be in the range of 8-12 nm and is in good agreement with the observed value from XRD. It is revealed from the TEM micrographs of pure and Ag admixed ZnO samples that the average particle size is noticeably large in the case of Ag admixed ZnO. The high-resolution TEM (HRTEM) provides further insights into the structure of Ag admixed ZnO NPs. *Fig. 5c* represents HRTEM micrograph of Ag admixed ZnO. The density of the nanocrystallites is higher at grain boundaries (GBs) in

compression to that within pure ZnO. Such a preferential presence of nanocrystallites at grain boundaries may be understood in terms of interaction of GB with ZnO/Ag admixed nanoparticles. The GBs are disordered regions in polycrystals and represent high energy configurations. Because of the Coulomb interaction between GB and the impurity atoms, the former attracted the later in order to decrease its energy.
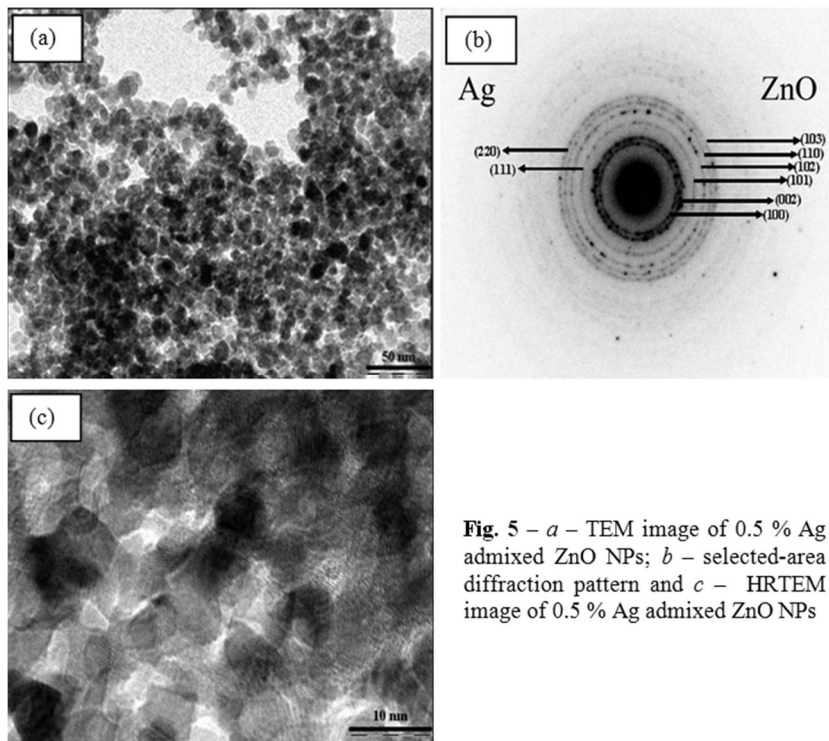

Fig. 5 – *a* – TEM image of 0.5 % Ag admixed ZnO NPs; *b* – selected-area diffraction pattern and *c* – HRTEM image of 0.5 % Ag admixed ZnO NPs

The diffusion of Ag may take place at intergrain as well as intragrain sites, namely, at the GB and inside ZnO grains. The diffusion of Ag to the GB forming Ag admixed ZnO is easy because it will be quite difficult for Ag to diffuse into the grains because of the difference in sizes of Ag and Zn atoms. The SADP in Fig. 5(b) corresponding to the TEM micrograph reveals the spotty rings pattern of [10.0], [00.2], [11.0] and [10.1] diffraction planes of ZnO & [111] and [220] diffraction planes of Ag. These diffraction rings correspond to ZnO/Ag nanoparticles.

A facile solution route, free from the use of surfactants has been developed to synthesize the ZnO NPs and Ag admixed ZnO NPs in the presence of

NaOH. The synthesis has been carried out at low temperature 70 °C for the short duration of 1 hr. The size of the nanoparticles is found to increase with the increase in Ag (0.5 to 1 at. %) content. Large blue-shifts relative to the bulk exciton absorption of ZnO are observed in the absorption and PL spectra of the pure and Ag admixed ZnO samples. The emission intensity of PL spectra of Ag admixed ZnO sample was been found to decrease considerably with respect to that of pure sample. NaOH plays multiple roles in the formation of pure ZnO NPs and Ag admixed ZnO NPs. It serves not only as reducing agent but also as a complexing agent and molecular template.

REFERENCES

[1] A.P. Alivisatos, Science, 1996, Vol. 271, P.933.
[2] I.G. Valls, M.L. Cantu, Energy Environ. Sci., 2009, Vol. 2, P.19.
[3] G. Shen P.C. Chen, K. Ryu, C. Zhou, J. Mater. Chem., 2009, Vol. 19, P.828.
[4] C. Klingshirn, Phys. Stat. Sol. (b), 2007, Vol. 244, P.3027.
[5] J. Singh, S.S. Patil, M.A. More, D.S. Joag, R.S. Tiwari, O.N. Srivastava, Appl. Sur. Sci., 2010, Vol. 256, P.615.
[6] H.B. Zeng, W.P. Cai, P.S. Liu, X.X. Xu, H.J. Zhou, C. Klingshirn, ACS Nano, 2008, Vol. 232, P.1661.
[7] H.B. Zeng, P.S. Liu, W.P. Cai, S. Yang, X.X. Xu, J. Phys. Chem. C, 2008, Vol. 112, P.19620.
[8] Y.F. Zhu, D.H. Fan, W.Z. Shen J. Phys. Chem. C, 2008, Vol. 112, P.10402.
[9] Y.J. Tak, K.J. Yong, J. Phys. Chem. C, 2008, Vol. 112, P.74.
[10] Y.H. Zheng, C.Q. Chen, Y.Y. Zhan, X.Y. Lin, Q. Zheng, K.M. Wei, J. Phys. Chem. C, 2008, Vol. 237, P.10773.
[11] R. Georgekutty, M.K. Seery, S.C. Pillai, J. Phys. Chem. C, 2008, Vol. 112, P.13563.
[12] C. Pacholski, A. Kornowski, H. Weller, Angew. Chem. Int. Ed., 2004, Vol. 43, P. 4774.
[13] C.D. Gu, C. Cheng, H.Y. Huang, T.L. Wong, N. Wang, T.Y. Zhang, Cryst. Growth. Des. Vol. 241, 2009, P.3278.
[14] D.D. Lin, H. Wu, R. Zhang, W. Pan, Chem. Mater., 2009, Vol. 21, P.3479.
[15] R.H. Wang, J.H.Z. Xin, Y. Yang, H. F. Liu, L. M. Xu, J.H. Hu, Appl. Surf. Sci., 2004, Vol. 227, P.312.
[16] V.V. Nikesh, S. Mahamuni, Semicond. Sci. Tech., 2001, Vol. 16, P. 687.